EARTHQUAKE ENGINEERING AND STRUCTURAL DYNAMICS
Earthquake Engng. Struct. Dyn. **27**, 749–769 (1998)

THE DUCTILITY REDUCTION FACTOR IN THE SEISMIC DESIGN OF BUILDINGS

NELSON LAM*,†, JOHN WILSON‡ AND GRAHAM HUTCHINSON§
Department of Civil and Environmental Engineering, The University of Melbourne, Parkville 3052, Victoria, Australia

SUMMARY

This paper presents new trends in the relationship between the ductility reduction factor and the ductility demand in the seismic design of buildings. A total of 4860 inelastic time-history analyses were carried out to study this relationship using 60 single-degree-of-freedom models excited by an ensemble of 81 earthquake accelerogram records from around the world. The asymmetrical distribution of the results highlighted the inaccuracies associated with assuming a normal distribution simply described by the mean and standard deviation to represent the data. A probability of exceedence approach has been used based on counting the number of occurrences the ductility demand exceeds a specified level. The ductility reduction factors developed in this study are consistent with other studies in the long-period range but are different in the short-period range. The ductility reduction factor for very short period buildings of limited ductility has been found to be greater than previously predicted. © 1998 John Wiley & Sons, Ltd.

KEY WORDS: earthquake; seismic design; ductility; buildings

1. INTRODUCTION

Conventional seismic design procedures specified in most contemporary earthquake loading standards and codes, including the Uniform Building Code[1] (UBC) of the U.S.A. use elastic analyses to estimate earthquake-induced load effects on buildings. The earthquake loads are modified to account for the inelastic behaviour of the building using the structural response factor, or the design strength reduction factor (R), which is defined as the ratio

$$R = \frac{S_{\text{elastic}}}{S_{\text{design}}} \tag{1}$$

where S_{elastic} is the estimated elastic strength demand and S_{design} the design strength.

The UBC specifies R values for design purposes based on the structural form of the building. The R values have been developed from Californian research and experience and broadly account for the following characteristics of the structural system: energy absorbing capability, expected overstrength, likely degree of redundancy and performance in past earthquakes. A similar set of R values have been adopted in earthquake loading standards worldwide including areas where the nature of the seismic hazard and the construction practices are very different from California.

Analytical methods have also been used to justify the strength reduction factor which is considered to be partly attributed to the system's ductility and partly to the increase in strength as a result of strain hardening

* Correspondence to: Nelson Lam, Department of Civil and Environmental Engineering, The University of Melbourne, Parkville 3052, Victoria, Australia
† Research Fellow
‡ Senior Lecturer
§ Professor of Civil Engineering and Head of Department

CCC 0098–8847/98/070749–21$17·50

Received 18 August 1997
Revised 6 January 1998

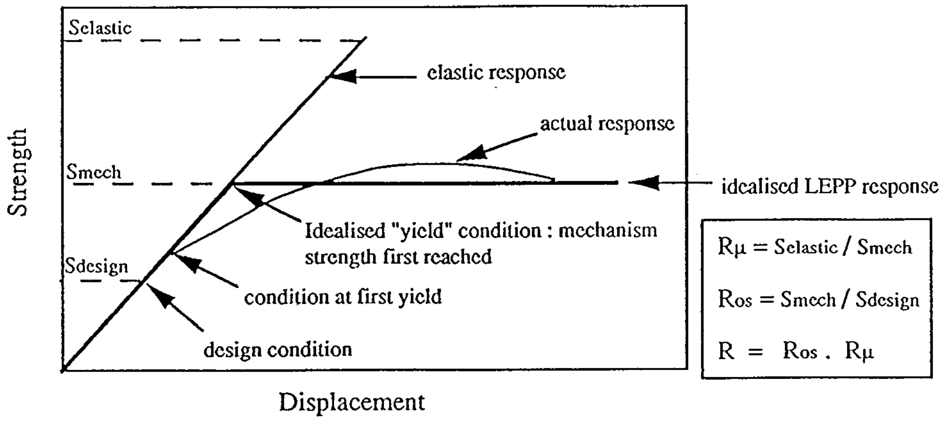

Figure 1. Strength reduction factors assuming LEPP behaviour

and plastic hinge formation.[2] Thus, R is often expressed as

$$R = R_{\mu} \cdot R_{\mathrm{OS}} \tag{2}$$

where R_{μ} is the ductility reduction factor and R_{OS} is the overstrength factor (refer Figure 1). R_{μ} is defined as

$$R_{\mu} = \frac{S_{\mathrm{elastic}}}{S_{\mathrm{mech}}} \tag{3}$$

where S_{mech} is the building's actual lateral mechanism strength which can be estimated by a monotonic quasi-static push-over analysis. Thus, R_{μ} takes into account the difference between the effect of a sustained (or static) load and an earthquake induced reversible dynamic load.

Similarly, R_{OS} is defined as

$$R_{\mathrm{OS}} = \frac{S_{\mathrm{mech}}}{S_{\mathrm{design}}} \tag{4}$$

Newmark and Hall[3] related R_{μ} to the kinematic ductility demand μ by the following expressions:

$$R_{\mu} = \begin{cases} \mu & (\text{for } T > 0{\cdot}5\,\mathrm{s}) \\ \sqrt{2\mu - 1} & (\text{for } 0{\cdot}1 < T < 0{\cdot}5\,\mathrm{s}) \\ 1 & (\text{for } T < 0{\cdot}03) \end{cases} \tag{5a–c}$$

which are based on the 'equal displacement' [equation (5a)], 'equal energy' [equation (5b)] and 'equal acceleration' [equation (5c)] propositions (refer Figure 2).

The Inelastic Design Response Spectrum (IDRS) can be approximately obtained by dividing the Linear Elastic Design Response Spectrum (LEDRS) by the product of R_{OS} and R_{μ} for each of the period ranges recommended in equation (5).

This Newmark–Hall procedure has been the most well known and widely used analytical method in the aseismic design of ductile structural systems. However, the phenomena embraced in the procedure was only justified on the basis of the response to simple displacement pulses.[3] In a follow-up study by Mahin and Bertero[4] using five Californian accelerogram records, significant scatter in the results was observed which challenged the accuracy of the R_{μ}–μ relationships assumed in the Newmark–Hall procedure.

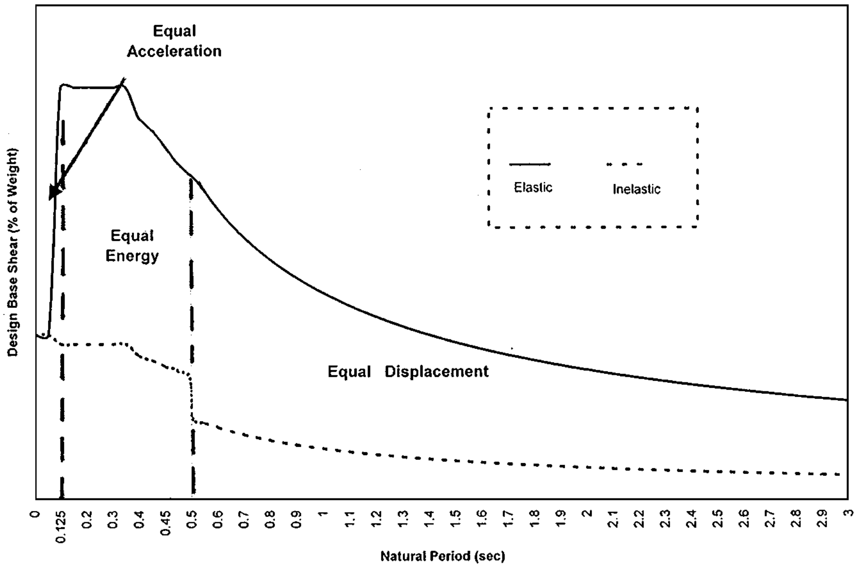

Figure 2. Newmark–Hall's inelastic design response spectrum

Simple SDOF systems were used to model the buildings in these studies. Higher-mode effects were therefore neglected and the results were only applicable to buildings in which the mode shape did not change significantly with yielding. Further, linear elasto-perfectly plastic (LEPP) hysteretic behaviour was assumed as it had been found that stiffness degradation and the shape of the hysteretic loop would not significantly affect the inelastic response behaviour,[4,5] provided the mechanical strength of the building did not deteriorate under cyclic loading.

2. RECENT DEVELOPMENTS

Similar analytical studies have been carried out in recent years by other researchers using a large ensemble of earthquake records to investigate both the ductility reduction factors and the inelastic design response spectra.[8–14] These analyses employed accelerograms recorded on rock, alluvial and soft soil sites and demonstrated the significant effect the predominant site period (i.e. the ground-motion-frequency content) has upon the ductility demand. By applying standard curve-fitting techniques to the ductility demand results, various period-dependent non-linear and piecewise linear relationships between R_μ and μ were obtained. (Reference 13 contains an excellent summary of studies carried out in the last 30 years on this subject.) The R_μ factor defined in the 'Displacement-based seismic assessment procedure' developed recently by Priestley[6,7] for reinforced concrete buildings takes into account the effect of the predominant site period as expressed in equation (6) (refer Figure 3):

$$R_\mu = 1 + (\mu - 1) = \frac{T}{1{\cdot}5\,T_g} \leqslant \mu \tag{6}$$

where T is the natural period of SDOF model and T_g the predominant site period.

Equation (6) assumes that 'Equal Displacement' proposition ($R_\mu = \mu$) applies when $T > 1{\cdot}5T_g$ and that 'Equal Acceleration' proposition ($R_\mu = 1$) applies when T approaches zero. Within these two limits R_μ is obtained by interpolation.

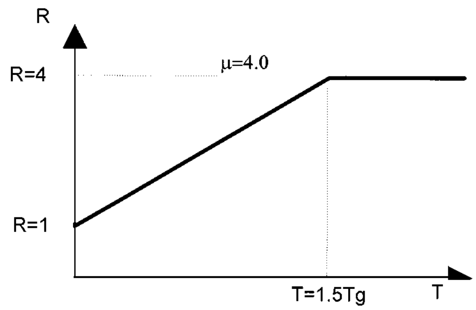

Figure 3. Priestley's strength reduction factor

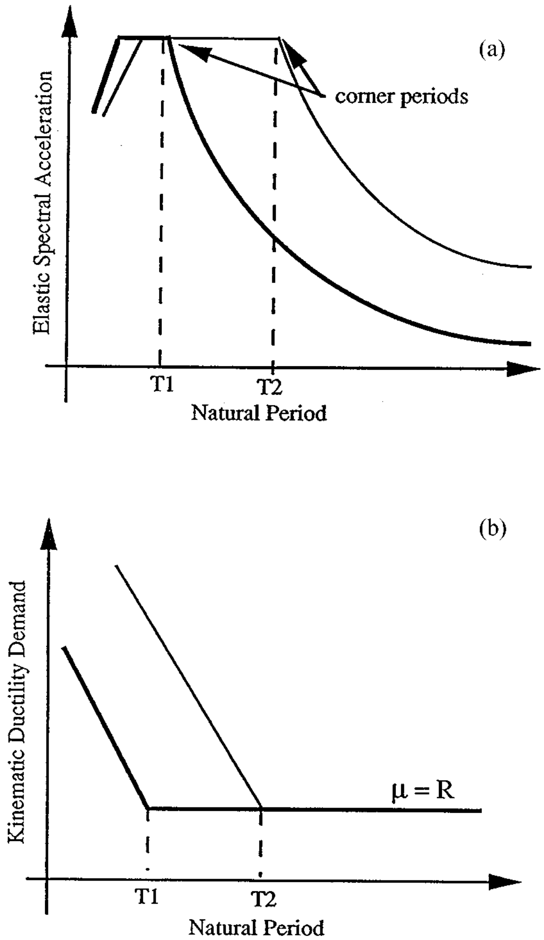

Figure 4. Corner period in the elastic response spectrum and the ductility demand spectrum

In a recent study by the authors,[15,16] analyses were carried out on SDOF models using 180 random phase-angle artificially generated accelerograms and 81 recorded strong motion accelerograms collected from different regions worldwide. The Corner Period introduced in this study[16] was equivalent to the 'predominant site period' or 'predominant period of ground motion' used by Miranda.[9,11] The Corner

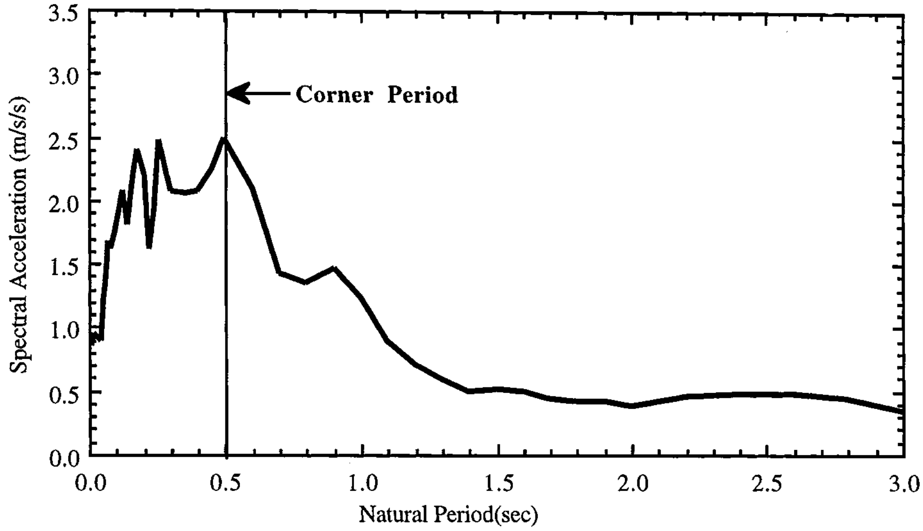

Figure 5. Corner period in the elastic response spectrum of a recorded accelerogram

Period associated with a codified model design response spectrum, is defined as the natural period at which the curved and the constant parts of the acceleration spectrum intersect [Figure 4(a)]. For a real spectrum, the Corner Period is the period at which the peak spectral acceleration occurs (Figure 5). If there is more than one dominant peak, the peak at the longer period is taken as the Corner Period since this is also the peak associated with the corresponding Relative Velocity Spectrum.[11] Importantly, the Corner Period of the ductility demand spectrum [Figure 4(b)] was consistent with the Corner Period of the corresponding elastic response spectrum [Figure 4(a)] confirming the findings by Miranda[11] and Riddell[12] that the ductility demand and the ground motion frequency content were strongly correlated.

The earthquake duration and phase angle effects on the ductility demand have also been studied in addition to the frequency content effects as described previously.[15] Ductility demand and damage levels associated with the elasto-perfectly plastic models were shown to be insensitive to the excitation duration. However, this result was not consistent with the observed damage levels in the field where duration was clearly important,[17] suggesting the direct correlation between strength degradation and earthquake duration. There was also little evidence to suggest any systematic influence of the phase-angles on ductility demand, implying that earthquakes with similar elastic response spectra (similar frequency content) but with different details of fault rupture and wave path can result in similar ductility demands.

Analysis results based on artificially generated accelerograms were generally consistent with those based on real accelerogram records although some discrepancies were observed when the frequency content was not accurately represented.[15]

3. DESCRIPTION OF THE PARAMETRIC STUDY

3.1. Aim of the study and analysis approach

The studies described above provide insight into the influence of various factors on ductility demand, but to date probabilistic treatment of the data has been generally limited. In this study, a large strong motion database has been used to facilitate a more elaborate statistical treatment of the data. The direct aim of this study is to develop a generalised R_μ–μ relationship for linear elasto-perfectly plastic (LEPP) SDOF systems

as a basis to rationalize seismic design provisions for codes of practices in both interplate and intraplate regions.

Two approaches can be applied to obtain correlations between R_μ and μ. In the first approach, inelastic analyses are carried out with a pre-determined value of R_μ to determine the ductility demand μ for each model. However, the inelastic response of structures to earthquake excitation is highly non-linear and is associated with considerable scatter.[9] The alternative approach determines directly the values of R_μ required to achieve several specified ductility values using an iterative procedure.

In the investigation described in this paper, the first approach has been adopted since it is considered essential to study the statistical properties of the asymmetrically distributed ductility demand data for different values of R_μ. Smooth correlations between the median and mean values of R_μ and μ have been obtained as demonstrated later in the paper.

Previous studies (described in Section 2) employing standard curve-fitting techniques implicitly assumed that the ductility demand was normally distributed, with the distribution conveniently represented by the mean and the standard deviation. These parameters, though commonly used, could be misleading should the distribution be asymmetrical or characterized by a cluster of outlying data points. In this study, the distribution of the results data was analysed by counting the number of occurrences in which particular ductility levels were exceeded. The median ductility level (for 50 per cent exceedence) together with ductility levels corresponding to other percentages of exceedence have been used to represent the distribution of ductility demand data.

3.2. Single-degree-of-freedom models

Sixty LEPP-SDOF models were created with different natural periods, T, and different yield strengths, S_y. The natural periods used were: 0·1, 0·2, 0·3, 0·4, 0·5, 0·6, 0·8,1·0, 1·2 and 1·6 s. The value of S_y (or S_{mech}) was calculated for each model using equation (3) with the assumed values of R_μ and S_{elastic}. R_μ values of 1·5, 2·0, 2·5, 3·0, 3·5 and 4·0 were input in turn whilst R_{OS} was assumed equal to unity (i.e. zero overstrength). Analyses were carried out separately for each model and each ground motion to determine the individual elastic strength demands, S_{elastic}.

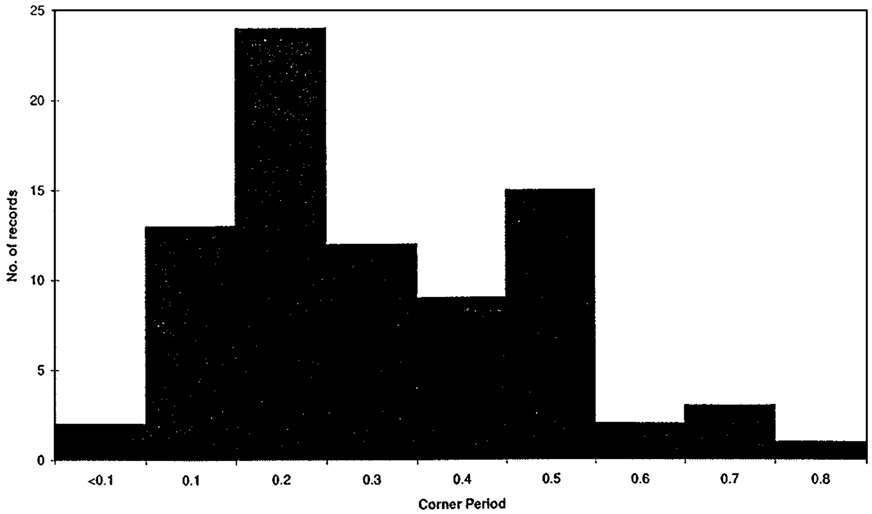

Figure 6. The dominant site period (or corner period) of the earthquake accelerograms in the database

3.3. Accelerograms used for the analyses

The earthquake database employed in this study contained 81 strong motion accelerogram records obtained from both interplate and intraplate regions around the world. In particular, it comprised records from the strike-slip fault region of Western North America, the subduction region of Central America and the Western Pacific, the collision regions of Southern Europe and the Middle East, and the intraplate regions of Australia, Eastern Canada and Central Canada. Earthquakes in the database measured above 5·5 on the Richter scale and were recorded within 60 km of the epicentre on a range of soil conditions including 'rock', 'stiff', 'intermediate' and 'soft'. Reference 15 by the authors contains a detailed description of each earthquake record including the peak ground acceleration and duration. The peak ground accelerations were typically between 0·1 and 0·6 g, whilst the frequency content (defined by the 'corner period' T_g (refer Figures 4 and 5)) was generally in the range 0·1–0·5 s, although with some records T_g reached 0·8 s (refer Figure 6).

4. PRELIMINARY OBSERVATIONS AND PARTITIONING OF THE DATA

A total of 4860 analyses were carried out with each model analysed in the elastic and the inelastic range using the earthquake accelerograms described above. The kinematic ductility demand ratio, μ, which is defined as the maximum inelastic displacement divided by the 'yield' displacement was determined for each analysis.

In Figure 7, the analyses results were plotted against the period ratio T/T_g for the ductility reduction factor of $R_\mu = 2{\cdot}5$. The results generally clustered in the range $\mu = 1$–5 except at very low values of T/T_g where a much larger ductility demand was observed. Figure 7 was then nominally divided into the 'short period', the 'medium period' and the 'long period' zones to group the data for statistical analyses. The division between the long and the medium period zone was nominally set at $T/T_g = 1{\cdot}5$ based on equation (6) and Figure 3. The division between the short and the medium period zones at around $T/T_g = 0{\cdot}6$ was based on a noticeable abrupt change in the ductility demand as observed in Figure 7. It is emphasized that the 'short',

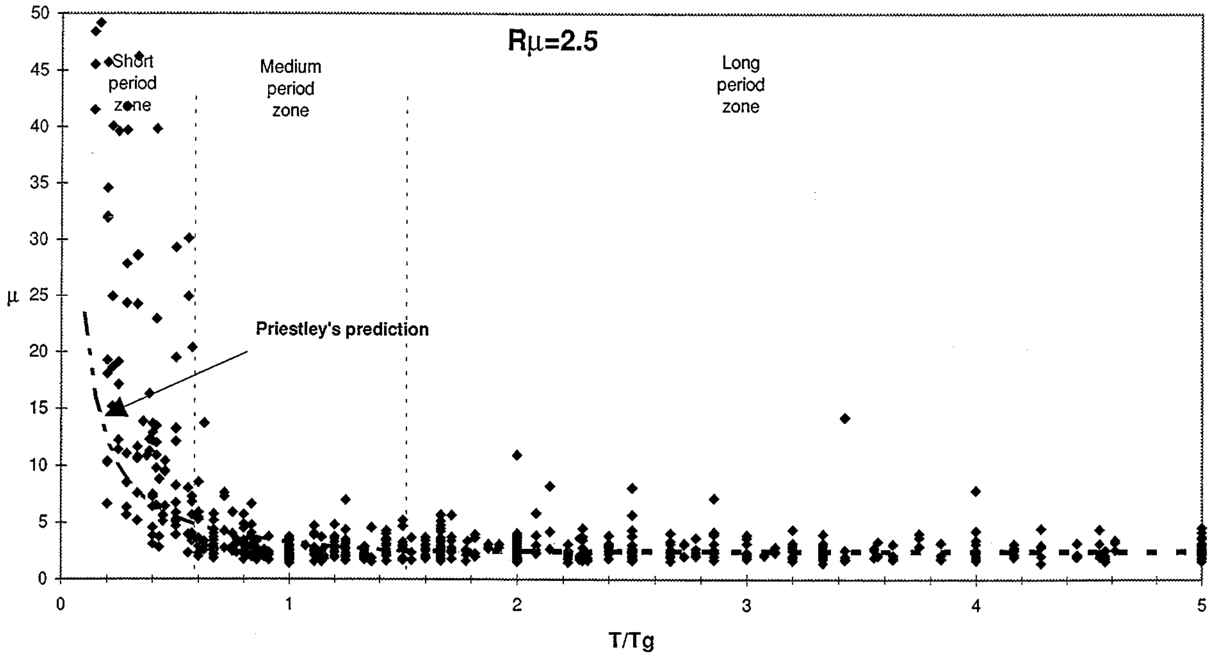

Figure 7. Ductility demand ratio versus period ratio ($R_\mu = 2{\cdot}5$)

'medium' and 'long' period zones as defined above should not be confused with similar terminology used in identifying the 'acceleration', 'velocity' and 'displacement' controlled parts of the elastic response spectrum.

The consistency of the data within each zone was evaluated by detailed analyses as shown in Figure 8(a)–(c). In Figure 8(a), the data in the range: $T/T_g = 0{\cdot}6$–$2{\cdot}5$ was divided into four sub-zones. In each sub-zone, the number of results exceeding $\mu = 2{\cdot}5$ (the equal displacement prediction) was counted. The percentage of exceedence was between 43 and 58 per cent which was in good agreement with the equal displacement prediction. A slight increase in the median ductility demand from $\mu = 2{\cdot}5$ to $2{\cdot}7$ can be seen as T/T_g approaches the short period zone of Figure 8(a). In addition to the statistical analysis of data in each zone, further analyses have been carried out to determine the median ductility demand for each value of T/T_g [refer dotted line in Figure 8(a)–(c)]. The median level generally fluctuated about the notional ductility level of 2·5, although a slightly higher ductility level was observed in the range $T/T_g = 0{\cdot}6$–$0{\cdot}8$.

Importantly, there was no indication that (in statistical terms) the ductility demand would vary significantly with the ratio T/T_g as suggested by equation (6) in the Medium-Period Zone.

Figure 8(b) and (c) further showed a very similar percentage of exceedence between sub-zones at the much longer period range. Overall, the data within the medium-period and the long-period zones was considered to be fairly consistent and further division into sub-zones was not deemed necessary.

At the period ratio in between the short- and the medium-period zones ($T/T_g = 0{\cdot}6$), a significant stepped increase in the ductility demand ratio μ from 2·7 to 12 was observed [Figure 9(a)]. This short-period zone was further divided into the ultra-short period and the medium-short period sub-zones. The percentage of results in the two sub-zones exceeding $\mu = 12$ was also very different, indicating that the ductility demand was highly period dependent. Significantly, the value of μ throughout the short-period zone significantly exceeded the ductility capacity of most building structures.

Ductility demand results associated with $R_\mu = 1{\cdot}5$ in the short period range have been presented in Figure 9(b), and importantly the percentage of results exceeding $\mu = 2$ was close to 50 per cent. This implies that ductility demand has been reduced to a level that can be accommodated in practice by a limited ductility structure.

The period zone divisions as shown in Figure 7 for $R_\mu = 2{\cdot}5$ appear reasonable whilst a review of the divisions for other R_μ values ($R_\mu = 1{\cdot}5$–4.0) has been summarized in Table I. Clearly, the critical T/T_g value dividing the short- and medium-period zones slightly increases as the ductility reduction factor R_μ increases, however, a conservative value of 2/3 may be assumed in practice.

Table II summarizes the number of analyses carried out in each zone for three different R_μ values, and clearly demonstrates that sufficient data were available for a meaningful statistical analysis of the results. A similar number of analyses were also carried out for $R_\mu = 2{\cdot}0$, 3·0 and 3·5.

5. STATISTICAL ANALYSIS OF RESULTS

The ductility demand obtained from the dynamic inelastic analyses were grouped according to the R_μ value and the period zone for statistical analysis and the results are presented and discussed in the following subsections [refer Figure 10(a)–(f)].

5.1. Mean, median, coefficient of variation and coefficient of skewness

Basic statistical properties, namely the mean, the median, the coefficient of variation and the coefficient of skewness have been examined for each period zone, and the observations are summarized as follows:

(a) *Mean ductility demand* [refer Figure 11(a)]. The mean ductility demand in the long-period zone was slightly above the 'equal displacement' prediction. The ductility demand in the medium-period zone was higher, but was well below the 'equal energy' prediction. The ductility demand in the short-period zone was well above both the 'equal displacement' and the 'equal energy' predictions.

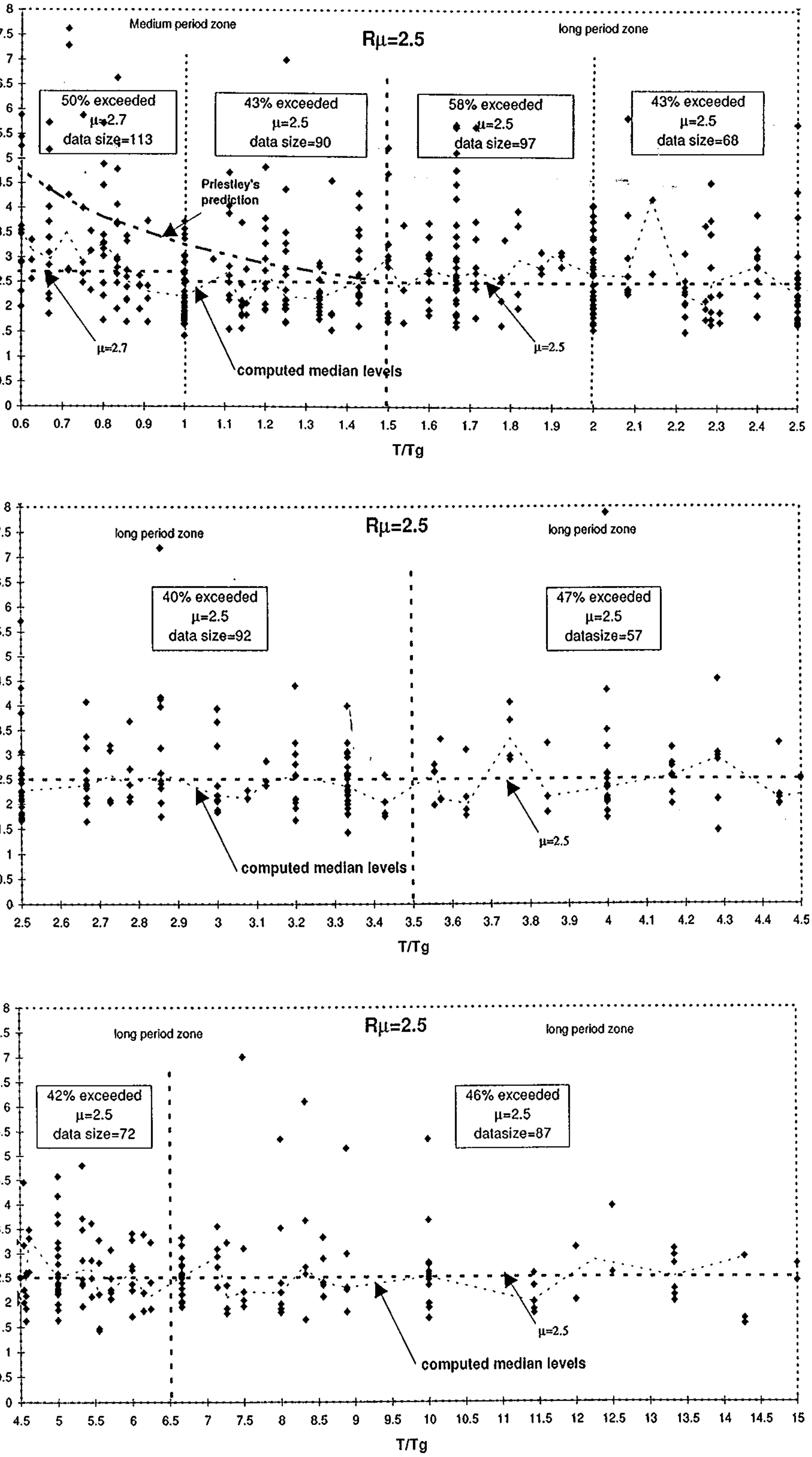

(a) (b) (c)

Figure 8. (a)–(c) Ductility demand ratio — consistency analyses in the long- and medium-period zones

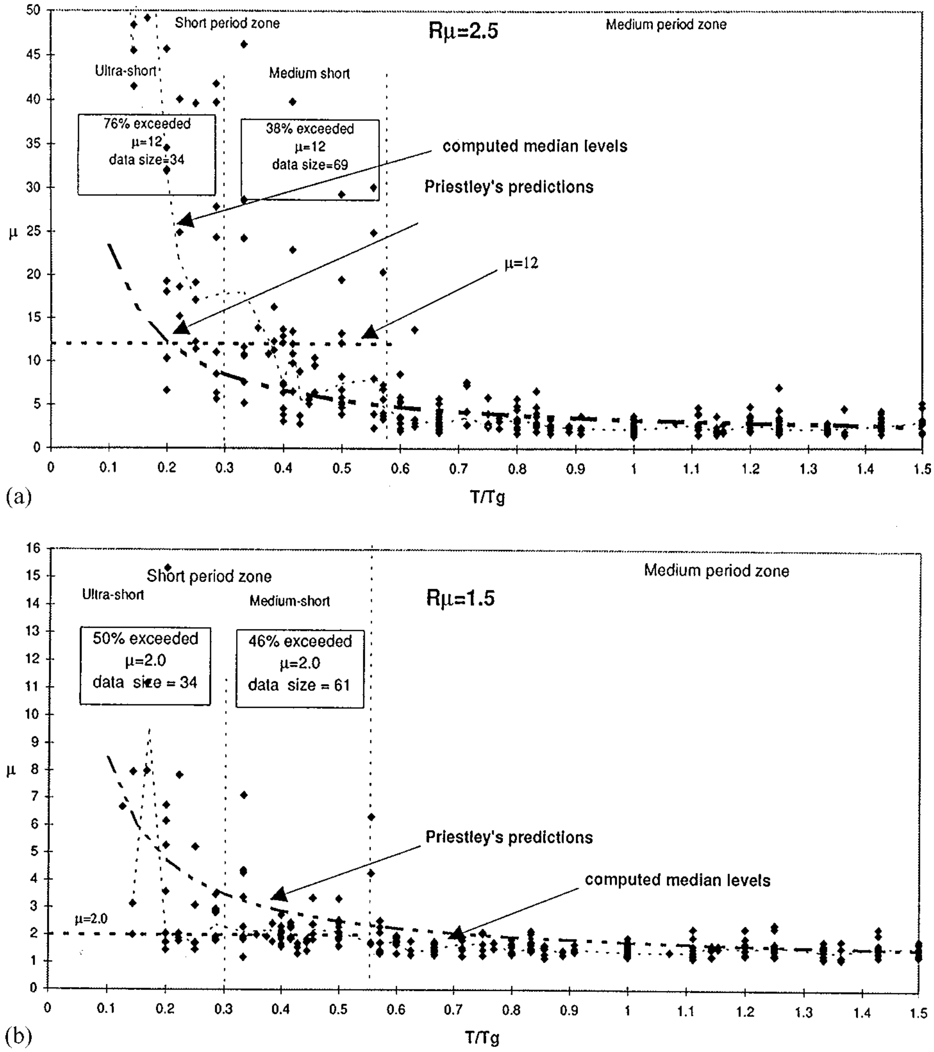

Figure 9. (a) and (b) Ductility demand ratio — consistency analyses in the short-period zones

Table I. T/T_g values separating the period zones

R_μ	T/T_g value in between the short- and the medium-period zones	T/T_g value in between the medium- and long-period zones
1·5	0·55	1·5
2·0	0·57	1·5
2·5	0·59	1·5
3·0	0·61	1·5
3·5	0·63	1·5
4·0	0·65	1·5

Table II. Number of analyses performed

Zones	$R = 1{\cdot}5$	$R = 2{\cdot}5$	$R = 4{\cdot}0$
Ultra-short	34	34	No zone sub-division
Medium-short	56	69	
Short	90	103	118
Medium	216	203	188
Long	504	504	504
Total	810	810	810

(b) *Median ductility demand* [refer Figure 11(b)]. The median ductility demand value in both the long- and the medium-period zones were very similar and were almost coincident with the 'equal displacement' prediction when $R_\mu \leqslant 2{\cdot}5$. Such similarities were not observed with the corresponding mean ductility demand. The median ductility demand values in the short-period zone were significantly higher than the longer period zones, and importantly were much less than the mean ductility demand particularly when $R_\mu \leqslant 1{\cdot}5$.

(c) *Coefficient of variation* (COV) [refer Figure 11(c)]. The COV of the ductility demand obtained in the long- and the medium-period zones were similar, and both increased gradually as R_μ increased (i.e. yield strength reduced) reflecting an increased scatter in the results. The COV of the short-period zone was much higher than the other two zones.

(d) *Coefficient of skewness* (CSK) [refer Figure 11(d)). CSK indicates the amount of skew in a distribution, as defined by equation (7):[13]

$$\mathrm{CSK} = \frac{3\ (\text{mean} - \text{median})}{\text{standard deviation}} \tag{7}$$

The distribution of the results in all zones were significantly skewed, with the skewness increasing as the natural period reduced and the R_μ value increased. Near symmetrical distributions were only found for the long-period zone and for very small values of R_μ.

5.2. Comparison with normal distribution

Statistical parameters such as the mean and the standard deviation can be misleading in a highly skewed distribution. To demonstrate this, the cumulative probability of exceedence of the analyses results (for $R_\mu = 1{\cdot}5$, $2{\cdot}0$ and $4{\cdot}0$) were compared to that of the theoretical normal distribution [refer Figure 12(a)–(c)]. The probability of exceedence is plotted against the dimensionless 'normal deviate' μ_Z[18] which is defined as

$$\mu_Z = \frac{\mu - \mu_{\text{mean}}}{\mu_{\text{standard deviation}}} \tag{8}$$

In a normal distribution, $\mu_Z = 0$ corresponds to the 'mean' ductility demand in which the cumulative probability of exceedence equals 50 per cent, and $\mu_Z = 1{\cdot}0$ corresponds to the 'mean plus one standard deviation' ductility demand in which the cumulative probability of exceedence equals 16 per cent. (Note that individual graphs in the same figure were normalized with respect to their own mean and standard deviation, and hence only the shapes and not the absolute values of the distribution were compared.)

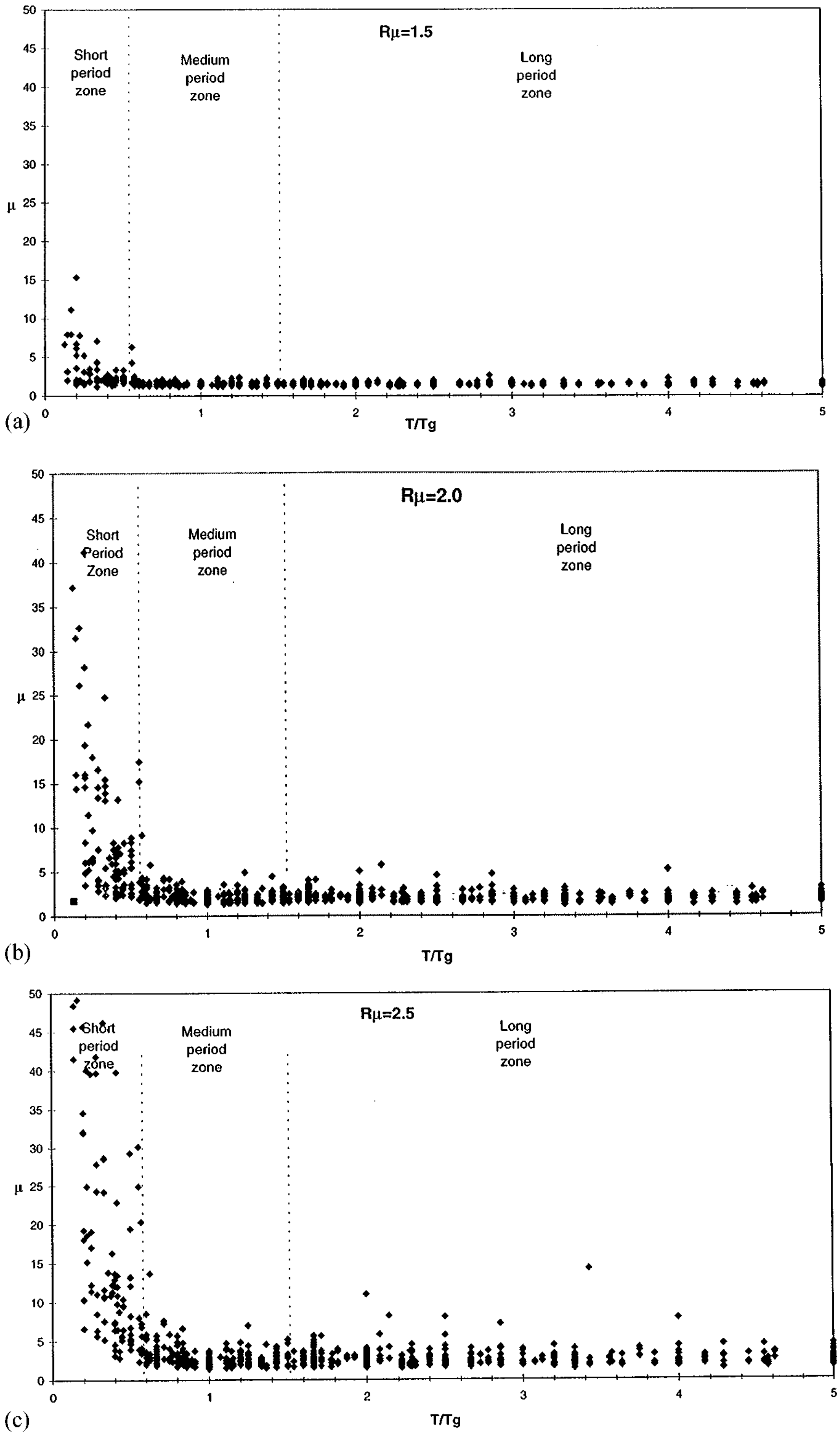

Figure 10. (a)–(c) Ductility demand ratio versus period ratio ($R_\mu = 1{\cdot}5$–$2{\cdot}5$)

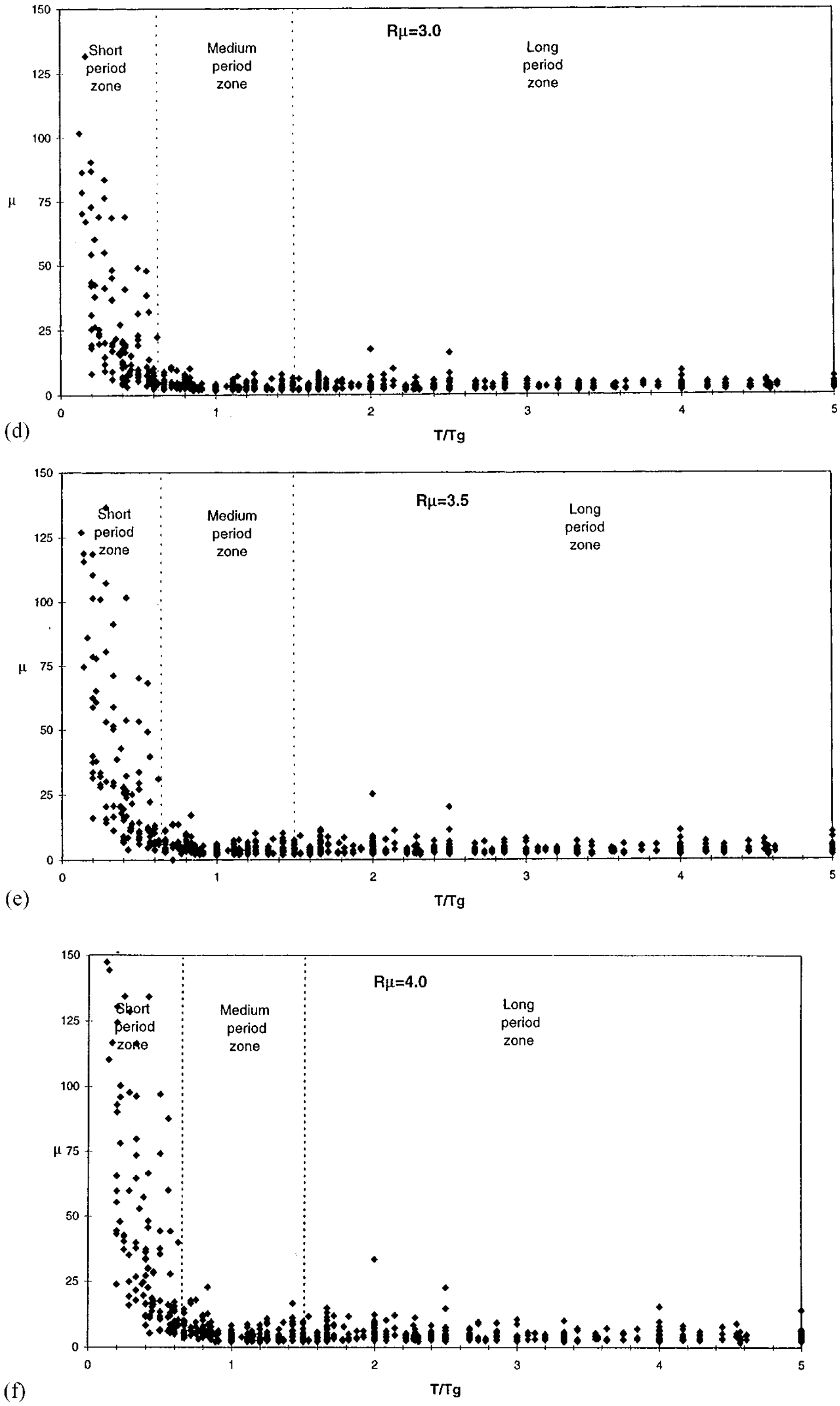

Figure 10. (d)–(f) Ductility demand ratio versus period ratio ($R_\mu = 3{\cdot}0$–$4{\cdot}0$)

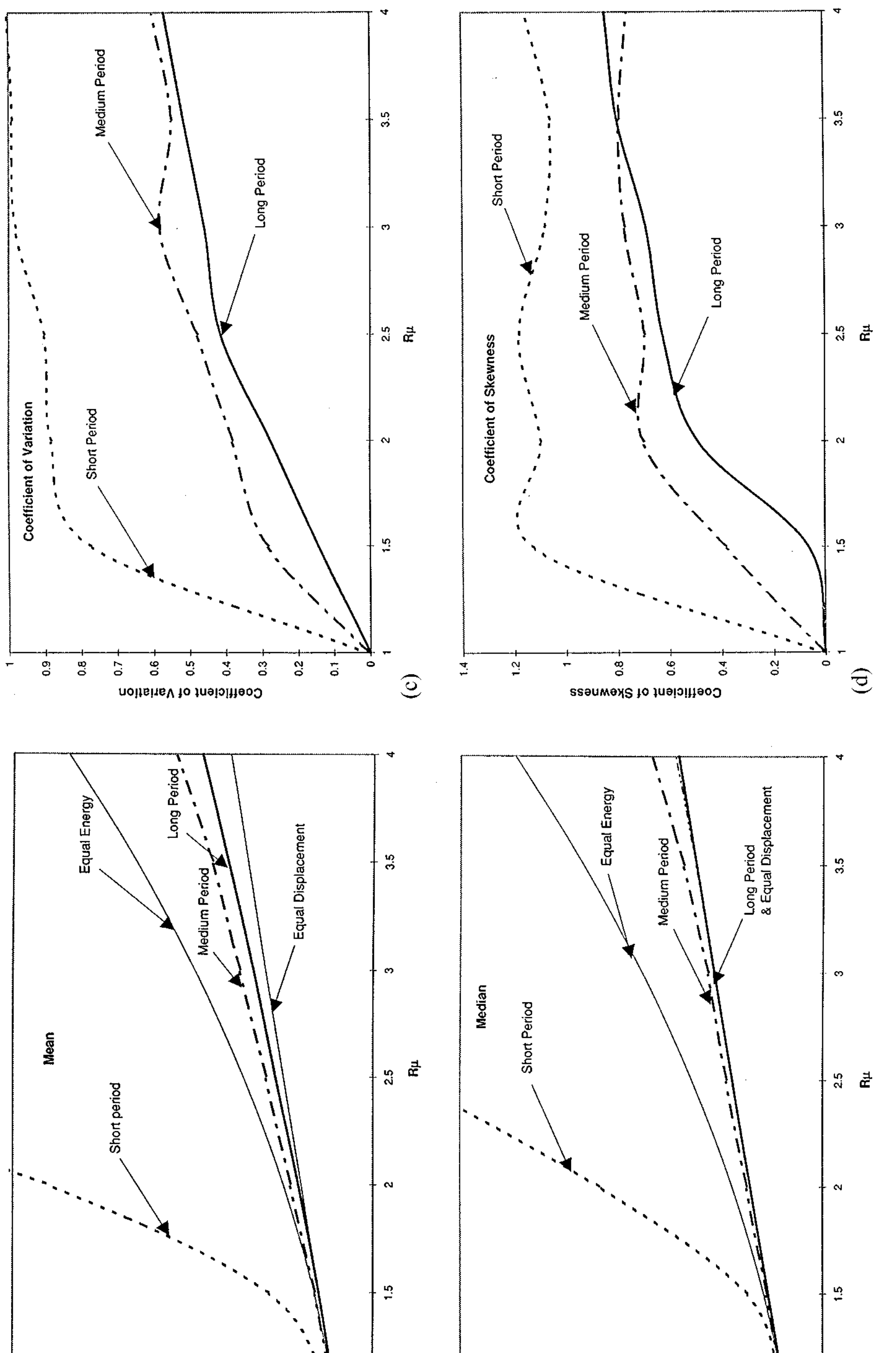

Figure 11. (a)–(d) Statistical properties: (a) mean, (b) median, (c) coefficient of variation and (d) coefficient of skewness

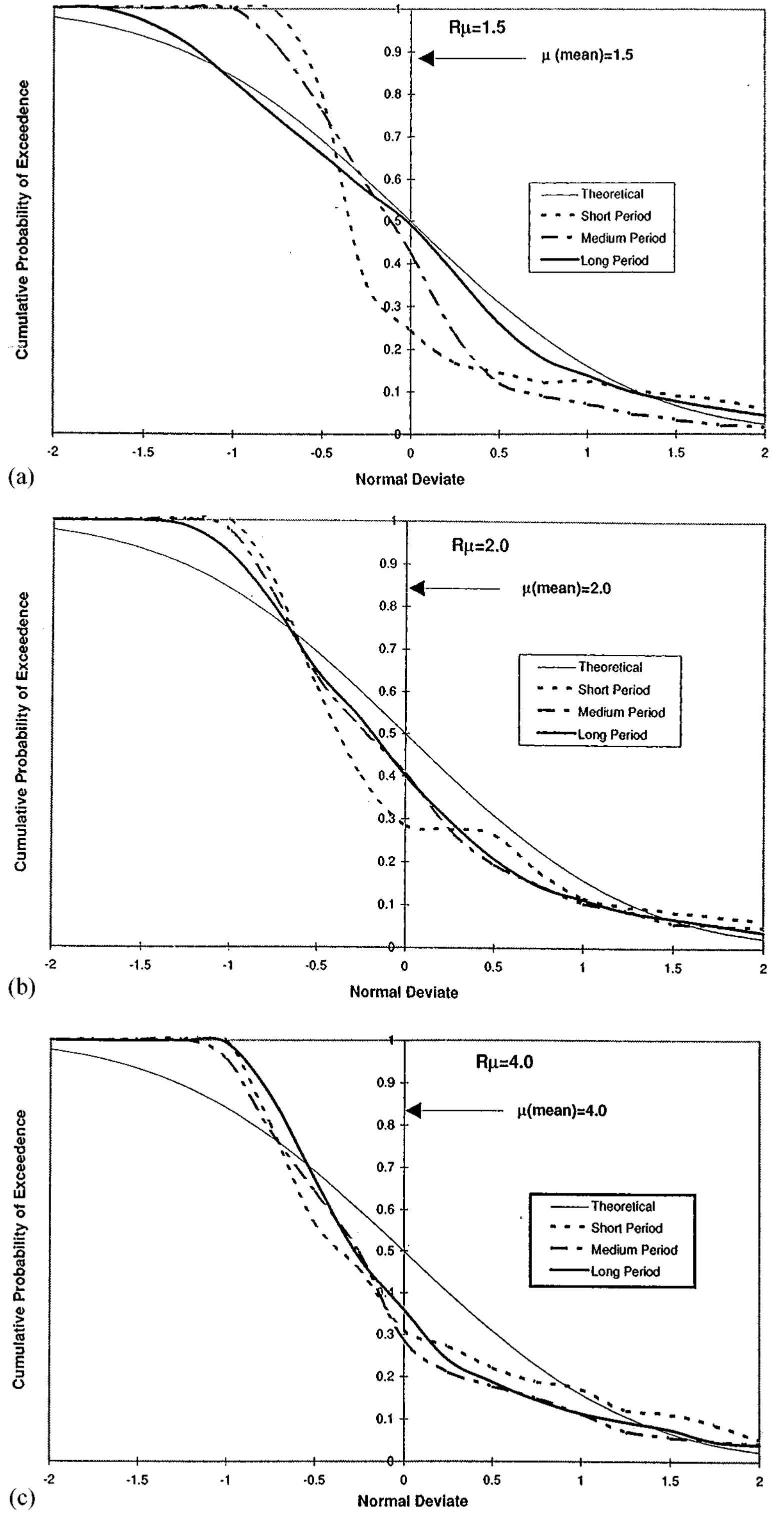

Figure 12. (a)–(c) Comparison with normal distribution

For $R_\mu = 1{\cdot}5$ [refer Figure 12(a)], the distribution of the results in the long-period zone were almost coincident with the theoretical distribution, but significant deviations were found in other period zones. In the short-period zone, only about 25 per cent of the results exceeded the mean value, which indicated a significant skew in the distribution.

For higher values of R_μ [refer Figure 12(b) and 12(c)] the distribution of the results in different period zones were similarly significantly skewed, with only 30–40 per cent of the results exceeding the mean value.

5.3. Probability of exceedence

The above discussions demonstrates the problem of using only the mean and the standard deviation to characterize asymmetrically distributed results. A more accurate method which takes into account the actual statistical distribution would be to specify the ductility demand corresponding to a particular level of exceedence.

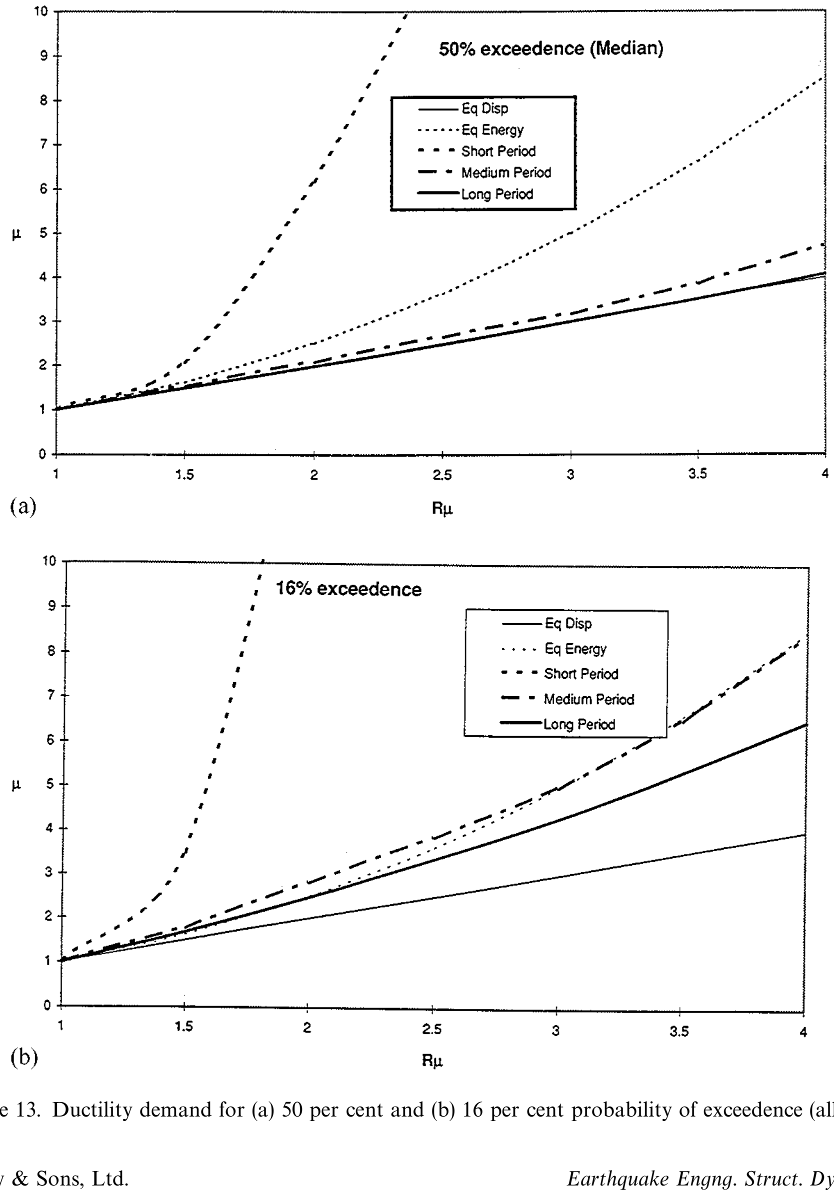

Figure 13. Ductility demand for (a) 50 per cent and (b) 16 per cent probability of exceedence (all zones)

The ductility demand corresponding to 16 and 50 per cent of exceedence is shown in Figures 13 and 14 for different period zones (16 per cent in a normal distribution corresponded to 'mean plus one standard deviation'). Importantly, the trends observed for different probability of exceedence values were very different due to significant skewness in the distribution of the ductility demand data. For example, the median ductility demand for the long- and the medium-period zones were very similar [refer Figure 13(a)], but the ductility demand of the two period zones corresponding to 16 per cent of exceedence deviated rather significantly from each other [refer Figure 13(b)]. Similar differences were further observed for the ultra-short and the medium-short period zones when $R_\mu \leqslant 1{\cdot}5$ [refer Figure 14(a) and 14(b)].

The foregoing discussion demonstrates the importance of choosing an appropriate percentage of exceedence for design. The choice depends on the nature of the hazard, the response of the structure (and the soil) to the hazard, and the acceptable risk of failure. Most contemporary codes of practice are based on an acceptable risk of failure of 10 per cent which corresponds to a 475 year return-period earthquake event for

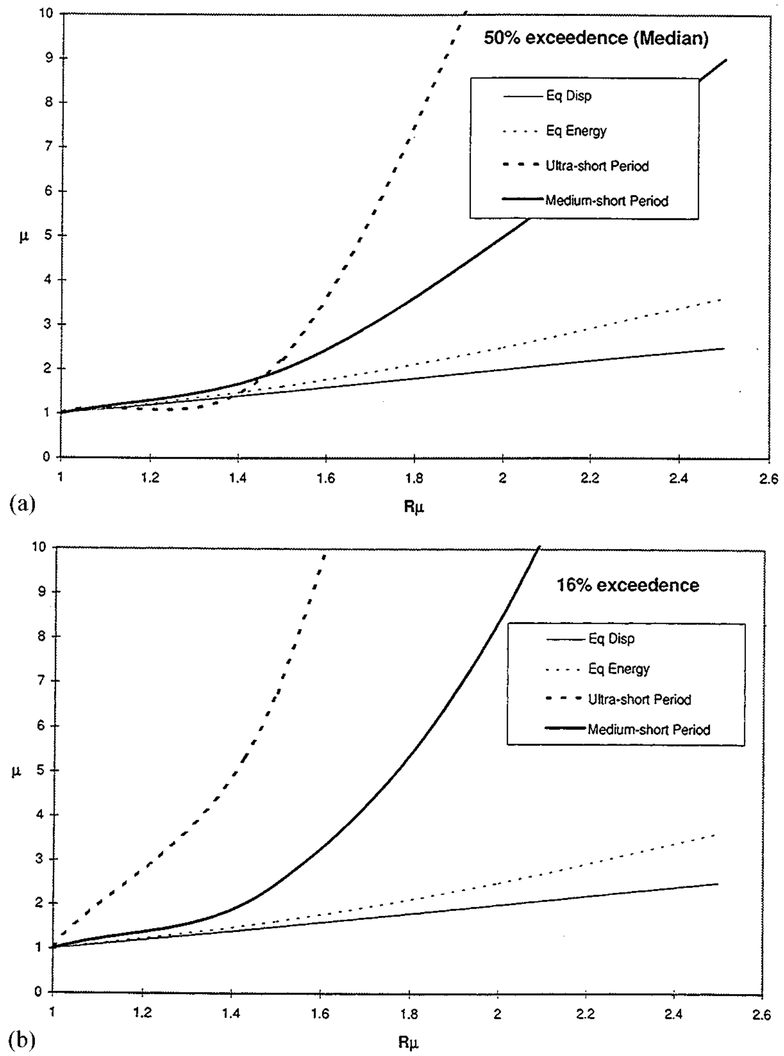

Figure 14. Ductility demand for (a) 50 per cent and (b) 16 per cent probability of exceedence (short period zones)

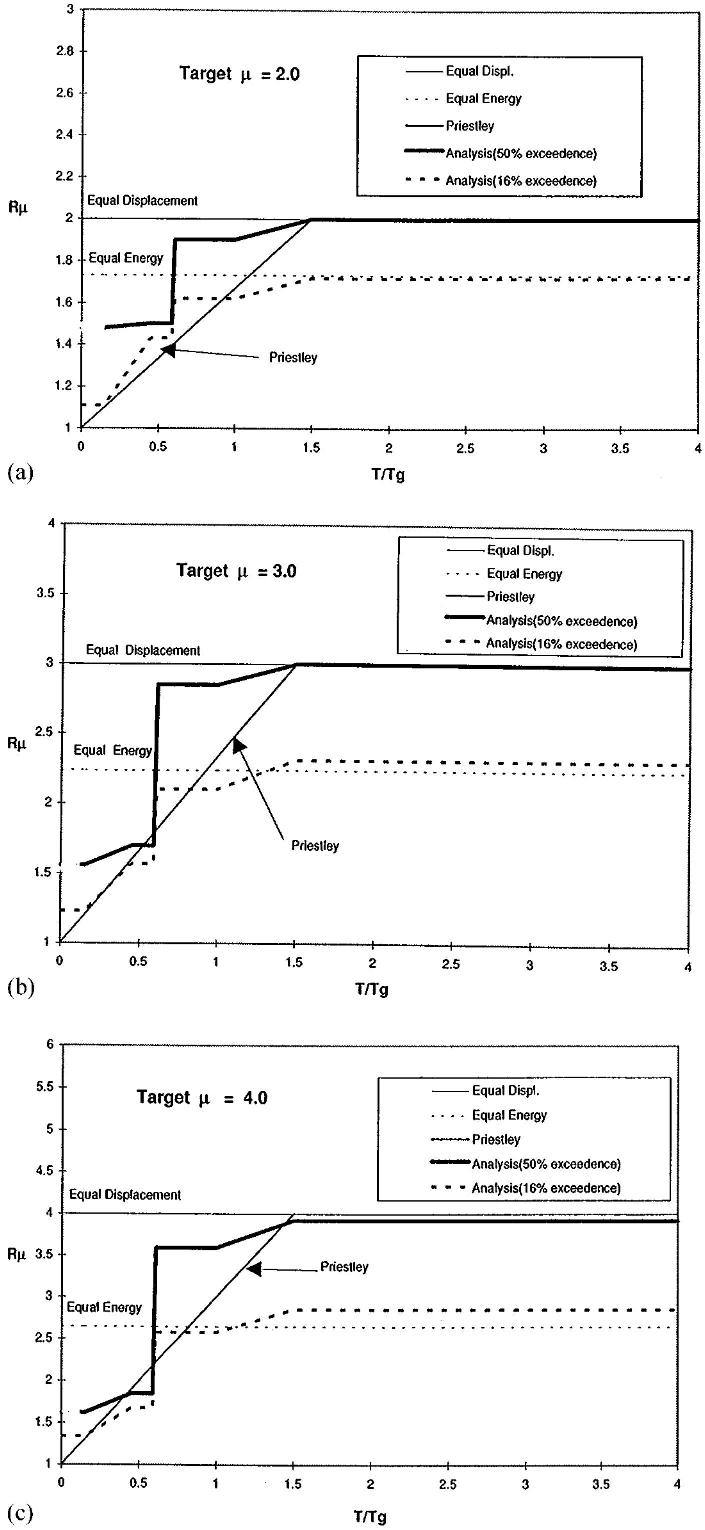

Figure 15. (a)–(c) Ductility reduction factors versus target ductility demand

a facility with a 50 year design life. However, it would be overconservative to design for the ductility demand corresponding to 10 per cent probability of exceedence in the results database, since the elastic force demand (based on coefficients provided by the seismic hazard map) will already have incorporated a safety margin. The recommended percentage of exceedence which should be used in determining the relationship between R_μ and μ is complex and is beyond the scope of this paper.

Whilst Reference 19 investigates this matter further, a probability of exceedence of 50 per cent (i.e. the median value) has been assumed in this paper.

6. DISCUSSION

The ductility demand μ, as a function of T/T_g and the ductility reduction factor R_μ can be summarized as follows:

(i) The median ductility demand in both the long- and medium-period zone was in good agreement with the equal displacement predictions.

(ii) The median ductility demand within both the long- and the medium-period zones appeared insensitive to changes in the T/T_g ratio.

(iii) A stepped change in the median ductility demand was observed within the range of $T/T_g = 0{\cdot}6$–$0{\cdot}7$ depending on the value of R_μ. In practice, the step may be conservatively assumed to occur at $T/T_g = 2/3$ for all values of R_μ.

(iv) Ductility demand in the short period zone was generally very high and significantly exceeded the ductility capacity of most buildings. However, the ductility demand was dramatically reduced when R_μ was lowered to 1·5.

The results from the analyses have been presented in Figure 15(a)–(c) in a form suitable for design purposes. These figures show the relationship between R_μ and T/T_g for target ductility values of $\mu = 2$, 3 and 4 for 50 and 16 per cent probability of exceedence. In addition, the R_μ values required according to the equal displacement, equal energy and Priestley's relationships have been plotted.

Priestley's piecewise linear relationship between R_μ, μ and T/T_g [equation (6)] is generally consistent with the observed data although some conservatism is apparent in the short-period zone.

Clearly, in the short-period zone ($T/T_g = 2/3$), ductility is generally no longer effective in reducing the design strength demand of a structure. However, a value of $R_\mu = 1{\cdot}5$ in the short period zone could result in a controllable ductility demand imposed on the structure under earthquake excitation and could be equivalent to an overall strength reduction factor R of about 2·25 since $R = R_{OS} R_\mu$ and R_{OS} is in the order of 1·5 ($R = 1{\cdot}5 \times 1{\cdot}5 = 2{\cdot}25$).

7. CONCLUSION

(i) Time-history analyses have been carried out on 60 LEPP-SDOF models with natural periods ranging between 0·1 and 1·6 s, and with the ductility reduction factors of between 1·5 and 4·0. An ensemble of 81 earthquake accelerograms, with different dominant site periods, obtained from different sources around the world were used for the analyses. Results from the analyses were grouped into short-period, medium-period and long-period zones. The critical T/T_g ratio dividing the short- and the medium-period zones was in the range 0·6–0·7 depending on the value of R_μ, however the adoption of a constant value of 2/3 is considered conservative.

(ii) The statistical distribution of ductility demand results was significantly skewed and resulted in only 30–40 per cent (instead of 50 per cent) of the results exceeding the mean value. For this reason, the use of the normal distribution defined by the 'mean' and 'standard deviation' is not considered appropriate to represent

the data. The ductility demand level corresponding to a defined probability of exceedence is considered more representative.

(iii) The median (50 per cent exceedence) ductility demand in the long- and medium-period zones was generally insensitive to changes in the period ratio T/T_g and was in good agreement with the equal displacement prediction. In contrast, a very high ductility demand was observed in the short-period zone.

(iv) Ductility is no longer effective in reducing the design strength demand of a structure when T/T_g is less than about 2/3. However, an overall structural response factor of $R = 2{\cdot}25$ (assuming an overstrength factor in the order of 1·5) would still result in a controllable ductility demand imposed on the structure.

(v) Priestley's expression [equation (6)] for the ductility reduction factor is generally consistent with the observed relationship although some conservatism is apparent in the short-period range.

APPENDIX

Notation

CK	coefficient of skewness
COV	coefficient of variation
R	structural response factor or design strength reduction factor
R_μ	ductility reduction factor
R_{OS}	overstrength factor
$S_{elastic}$	estimated elastic strength demand
S_{design}	design strength
S_{mech}	system's mechanism strength
S_y	yield strength
T	building model's natural period
T_g	corner period or dominant site period
$\frac{T}{T_g}$	period ratio

Greek letters

μ	kinematic ductility demand
μ_Z	normal deviate variable of the ductility demand

REFERENCES

1. Int. Conf. Building Officials, U.S.A., '*Uniform Building Code*', Division IV: Earthquake Design, 1997.
2. C. M. Uang, 'Establishing R (or R_W) and C_d factors for building seismic provisions', *J. Struct. Engng.* **117** (1), 19–28 (1991).
3. N. M. Newmark and W. J. Hall, 'Earthquake spectra and design', Engineering Monograph, Earthquake Engineering Research Institute, Berkeley, California, 1982.
4. S. A. Mahin and V. V. Bertero, 'An evaluation of inelastic seismic design spectra', *J. Struct. Div. A.S.C.E.* **107** (ST9), 1777–1795 (1981).
5. P. J. Moss, A. J. Carr and A. H. Buchanan, 'Seismic response of low-rise buildings', *Bull. New Zealand Natl. Soc. Earthquake Engng* **19**(3), 180–198 (1986).
6. M. J. N. Priestley, 'Displacement-based seismic assessment of existing reinforced concrete buildings', *Proc. Pacific Conf. on Earthquake Engineering*, University of Melbourne, Victoria, Australia, pp. 225–244, 1995.
7. M. J. N. Priestley, 'Displacement-based seismic assessment of reinforced concrete structures to NZS 4203:1992', *Paper presented to the Annual Technical Conf. of the New Zealand National Society for Earthquake Engineering*, New Plymouth, New Zealand, March 1996.
8. F. E. Elghadamsi and B. Mohraz, 'Inelastic earthquake spectra', *Earthquake Engng. Struct. Dyn.* **15**, 91–104 (1987).
9. E. Miranda, 'Evaluation of site-dependent inelastic seismic design spectra', *J. Struct. Engng., ASCE* **119**(5), 1319–1338 (1993).
10. H. Krawinkler and A. A. Nassar, 'Seismic design based on ductility and cumulative damage demands and capacities', in Fajfar and Krawinklers (eds), *Nonlinear Seismic Analysis and Design of Reinforced Concrete Buildings*, Elsevier Applied Science, New York, 1992.
11. E. Miranda, 'Site dependent strength reduction factors', *J. Struct. Engng., ASCE* **119**(12), 3505–3519 (1993).

12. R. Riddell, 'Building ductility demand: inelastic design spectra accounting for soil conditions', *Earthquake Engng. Struct. Dyn.* **24**, 1491–1510 (1995).
13. E. Miranda and V. V. Bertero, 'Evaluation of strength reduction factors for earthquake resistant design', *Earthquake Spectra* **10**(2), 357–379 (1994).
14. T. Vidic, P. Fajfar and M. Fischinger, 'Consistent inelastic design spectra: strength and displacement', *Earthquake Engng. Struct. Dyn.* **23**, 507–521 (1994).
15. N. T. K. Lam, J. L. Wilson and G. L. Hutchinson, 'Building ductility demand: interplate versus intraplate earthquakes', *Earthquake Engng Struct. Dyn.* **25**(9), 965–985 (1996).
16. N. T. K. Lam, J. L. Wilson and G. L. Hutchinson, 'The dependence of ductility demand on the frequency characteristics of earthquake ground motion', *Proc. 14th Australasian Conf. on the Mechanics of Structures and Materials*, University of Tasmania, Hobart, pp. 1995, pp. 290–295.
17. H. Tiedmann, *Earthquake and Volcanic Eruptions — A Handbook on Risk Assessment*, Swiss Reinsurance Company, Switzerland, 1992.
18. L. L. Lapin, *Probability and Statistics for Modern Engineering*, 2nd edn, PWS-Kent Publishing, Boston, MA (1990).
19. N. T. K. Lam, J. L. Wilson and G. L. Hutchinson, 'The influence of seismic hazard on the ductility reduction factor', Department of Civil and Environmental Engineering, The University of Melbourne, 1997.

